Applied Mathematics & Information Sciences
An International Journal

Right Triangular Spherical Dihedral f–Tilings with Two Pairs of Congruent Sides

Catarina P. Avelino and Altino F. Santos

Department of Mathematics, UTAD, 5001 - 801 Vila Real, Portugal

Received: 17 Aug. 2012, Revised: 22 Nov. 2012, Accepted: 13 Jan. 2013
Published online: 1 May 2013

Abstract: In this paper we present the study of dihedral f-tilings by spherical right triangles on two distinct cases of adjacency and with two pairs of congruent sides. Some aspects of the combinatorial structure are given.

Keywords: Dihedral f-tilings, combinatorial properties, spherical trigonometry.

1 Introduction

By a dihedral *folding tiling* (*f-tiling*, for short) of the sphere S^2 whose prototiles are spherical right triangles, T_1 and T_2, we mean a polygonal subdivision τ of S^2 such that each *cell* (*tile*) of τ is congruent to T_1 or T_2 and the vertices of τ satisfy the *angle-folding relation*, i.e., each vertex of τ is of even valency and the sums of alternating angles around each vertex are π. In fact, the crease pattern associated to the subjacent graph of a spherical f-tiling satisfy the Kawasaki's condition at any vertex v. In this paper we shall discuss dihedral f-tilings by spherical right triangles, considering two distinct cases of adjacency. We assume that from all the sides of the prototiles involved there are two pairs of congruent sides. The 3-dimensional representations of the obtained f-tilings are presented as well as the combinatorial structure.

f-tilings are intrinsically related to the theory of isometric foldings of Riemannian manifolds, introduced by S. A. Robertson [6] in 1977. The classification of f-tilings was initiated by Ana Breda [1], with a complete classification of all spherical monohedral f-tilings. Later on, in 2002, Y. Ueno and Y. Agaoka [10] have established the complete classification of all triangular monohedral tilings (without any restrictions on angles).

The study of dihedral f-tilings by spherical right triangles is a very extensive and exhaustive work and some particular cases were recently obtained in papers [4, 5]. A list of all dihedral f-tilings of the sphere by triangles and parallelograms including the combinatorial structure of each tiling can be found in [2]. Robert Dawson has also been interested in special classes of spherical tilings, see [7–9] for instance.

We shall denote by $\Omega(T_1, T_2)$ the set, up to an isomorphism, of all dihedral f-tilings of S^2 whose prototiles are T_1 and T_2.

From now on T_1 is a spherical right triangle of internal angles $\frac{\pi}{2}$, α and β, with edge lengths a (opposite to β), b (opposite to α) and c (opposite to $\frac{\pi}{2}$), and T_2 is a spherical right triangle of internal angles $\frac{\pi}{2}$, γ and δ, with edge lengths d (opposite to δ), e (opposite to γ) and f (opposite to $\frac{\pi}{2}$) (see Figure 1). We will assume throughout the text that T_1 and T_2 are distinct triangles, i.e., $(\alpha, \beta) \neq (\gamma, \delta)$ and $(\alpha, \beta) \neq (\delta, \gamma)$. The case $\alpha = \beta$ or $\gamma = \delta$ was analyzed in [4], and so we will assume further that $\alpha \neq \beta$ and $\gamma \neq \delta$.

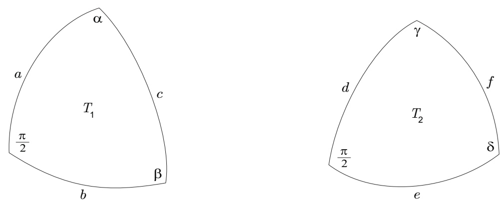

Fig. 1 Prototiles: spherical right triangles T_1 and T_2

Relations between faces, edges, vertices and angles of any dihedral f-tiling of S^2, with prototiles T_1 and T_2, are stated in proposition 1.

* Corresponding author e-mail: cavelino@utad.pt

Proposition 1.[3, Proposition 2.1] *Let $\tau \in \Omega(T_1, T_2)$. If $N_1 > 0$ and $N_2 > 0$ denote the number of spherical right triangles of τ congruent to T_1 and T_2, respectively, and E and V denote the number of edges and vertices of τ, respectively, then:*

(i) $N_1 + N_2 = 2V - 4 = \frac{2}{3}E \geq 8$;
(ii) $3V = 6 + E$;
(iii) there are, at least, six vertices of valency four;
(iv) the cases $(\alpha + \beta \geq \pi$ *and* $\gamma + \delta > \pi)$ *and* $(\alpha + \beta > \pi$ *and* $\gamma + \delta \geq \pi)$ *cannot occur.*

It follows straight away that

$$\alpha + \beta > \frac{\pi}{2} \quad \text{and} \quad \gamma + \delta > \frac{\pi}{2}, \tag{1}$$

and also $a \neq b$ and $d \neq e$.

In order to get any dihedral f-tiling $\tau \in \Omega(T_1, T_2)$, we find it useful to start by considering one of its *local configurations*, beginning with a common vertex to two tiles of τ in adjacent positions.

In the diagrams that follows it is convenient to label the tiles according to the following procedures:

(i) We begin the configuration of a tiling $\tau \in \Omega(T_1, T_2)$ with a right triangle T_1, labelled by 1; then we label with 2 a right triangle T_2, adjacent to T_1;
(ii) For $j \geq 3$, the location and orientation of tile j can be deduced from the configuration of tiles $(1, 2, 3, \ldots, j-1)$ and from the hypothesis that the configuration is part of a complete f-tiling (except in the cases indicated).

2 F–tilings by right triangles

In the following subsections we will consider separately two distinct cases of adjacency, assuming that any element of $\Omega(T_1, T_2)$ has at least two cells such that they are in adjacent positions and in one of the situations illustrated in Figure 2 (the remaining two cases of adjacency are not in the scope of this paper).

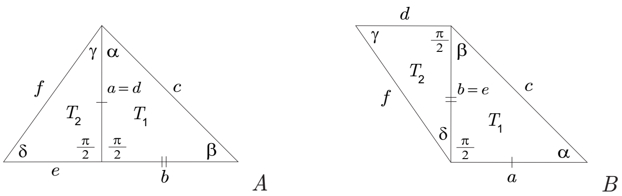

Fig. 2 Distinct cases of adjacency

We omit the analysis of the cases where all the edges of T_1 and T_2 have different lengths, except the adjacent sides. This study is very extensive and is outside of the scope of this work.

2.1 *Case of Adjacency A*

Suppose that any element of $\Omega(T_1, T_2)$ has at least two cells congruent, respectively, to T_1 and T_2, such that they are in adjacent positions as illustrated in Figure 2–A. We have $b \neq e$, as $b = e$ implies $T_1 \equiv T_2$. As $a = d$, using trigonometric formulas, we obtain

$$\frac{\cos\beta}{\sin\alpha} = \frac{\cos\delta}{\sin\gamma}. \tag{2}$$

In the following subsections we will consider separately the cases $a = c$, $b = c$, and $b = f$. Note that each one of the cases $a = f (= d)$ and $c = f$ imply $a = c$. The cases $e = f$ and $c = e$ are analogous to the cases $b = c$ and $b = f$ (the same f-tilings are obtained), respectively, where the roles of the angles (α, β) and (γ, δ) are interchanged.

2.1.1 $a = c$

The condition $a = c$ leads to $\beta = \delta = \frac{\pi}{2} = a = f$, $\alpha = b$ and $\gamma = e$.

Proposition 2.*If there are two cells in adjacent positions as illustrated in Figure 2–A, with $a = c$, then for each $k_1,\ k_2,\ \bar{k}_1,\ \bar{k}_2 \geq 1$, $\Omega(T_1, T_2) = \left\{\mathcal{P}^{\alpha}_{j_{(k_1,k_2)}}, \bar{\mathcal{P}}^{\alpha}_{\bar{j}_{(\bar{k}_1,\bar{k}_2)}}\right\}$, where $\mathcal{P}^{\alpha}_{j_{(k_1,k_2)}}$ and $\bar{\mathcal{P}}^{\alpha}_{\bar{j}_{(\bar{k}_1,\bar{k}_2)}}$, $\alpha \in \left(0, \frac{\pi}{2}\right)$, $\alpha \neq \gamma$, are non-isomorphic dihedral f-tilings, with $1 \leq j \leq \phi(k_1, k_2)$ and $1 \leq \bar{j} \leq \bar{\phi}(\bar{k}_1, \bar{k}_2)$, for some integers $\phi(k_1, k_2)$ and $\bar{\phi}(\bar{k}_1, \bar{k}_2)$, respectively; these values correspond to the number of distinct f-tilings in each class and satisfy $\phi(k_1, k_2) \leq \sum_{k=0}^{n} \binom{n}{k}^2$, with $n = k_1 + k_2$.*

Proof.

Suppose that any element of $\Omega(T_1, T_2)$ has at least two cells congruent, respectively, to T_1 and T_2, such that they are in adjacent positions as illustrated in Figure 2–A.

We will consider separately the cases $\alpha < \beta$ and $\alpha > \beta$.

1. Suppose firstly that $\alpha < \beta$. Consequently, $\alpha < \frac{\pi}{2}$, $\gamma \neq \alpha, \frac{\pi}{2}$. Therefore, the configuration illustrated in Figure 2–A is extended to the one given in Figure 3.

At vertices v_1 and v_2, that are in antipodal positions, we have

$$k_1\alpha + k_2\gamma = \pi \quad \text{or} \quad \frac{\pi}{2} + \bar{k}_1\alpha + \bar{k}_2\gamma = \pi,$$

$k_1,\ k_2,\ \bar{k}_1,\ \bar{k}_2 \geq 1$.

For each $\alpha \in \left(0, \frac{\pi}{2}\right)$, $\alpha \neq \gamma$, and each pair (k_1, k_2), with $k_1, k_2 \geq 1$, the condition $k_1\alpha + k_2\gamma = \pi$ leads to a class of f-tilings $\mathcal{P}^{\alpha}_{j_{(k_1,k_2)}}$, where $1 \leq j \leq \phi(k_1, k_2)$; $\phi(k_1, k_2)$ is the number of distinct f-tilings for the pair (k_1, k_2), and $2(k_1 + k_2)$ is the valency of the vertices v_1

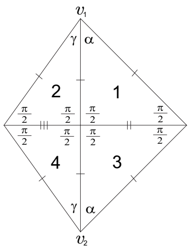

Fig. 3 Local configuration

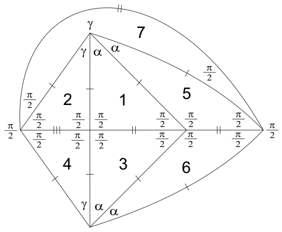

(a) Planar representation of $\mathcal{P}^{\alpha}_{1_{(1,1)}}$

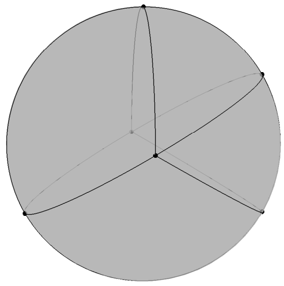

(b) 3D representation of $\mathcal{P}^{\alpha}_{1_{(1,1)}}$

Fig. 4 f-tiling $\mathcal{P}^{\alpha}_{1_{(1,1)}}$, $\alpha \in \left(0, \frac{\pi}{2}\right)$

and v_2. The value of $\phi(k_1, k_2)$ could be obtained counting circular permutations with two groups of indistinguishable objects. $\phi(k_1, k_2)$ satisfy $\phi(k_1, k_2) \leq \displaystyle\sum_{k=0}^{n} \binom{n}{k}^2$, with $n = k_1 + k_2$.

For instance, fixing $\alpha \in \left(0, \frac{\pi}{2}\right)$,

- if $k_1 = k_2 = 1$, there is a single f-tiling, $\mathcal{P}^{\alpha}_{1_{(1,1)}}$, whose planar and 3D representations are given in Figure 4;
- if $k_1 = 1$ and $k_2 = 2$, there are two distinct f-tilings, $\mathcal{P}^{\alpha}_{1_{(1,2)}}$ and $\mathcal{P}^{\alpha}_{2_{(1,2)}}$; planar and 3D representations are given in Figure 5 and Figure 6, respectively.

Similarly, the case $\frac{\pi}{2} + \bar{k}_1\alpha + \bar{k}_2\gamma = \pi$, with $\bar{k}_1, \bar{k}_2 \geq 1$, leads, for each $\alpha \in \left(0, \frac{\pi}{2}\right)$, $\alpha \neq \gamma$, and each pair $(\bar{k}_1, \bar{k}_2)$, to a class of f-tilings $\bar{\mathcal{P}}^{\alpha}_{\bar{j}_{(\bar{k}_1,\bar{k}_2)}}$, where $1 \leq \bar{j} \leq \bar{\phi}(\bar{k}_1, \bar{k}_2)$; $\bar{\phi}(\bar{k}_1, \bar{k}_2)$ is the number of distinct f-tilings for the pair $(\bar{k}_1, \bar{k}_2)$, and $2(\bar{k}_1 + \bar{k}_2 + 1)$ is the valency of the vertices v_1 and v_2. The value of $\bar{\phi}(\bar{k}_1, \bar{k}_2)$ could be obtained counting circular permutations with three groups of indistinguishable objects. For instance, the case $\bar{k}_1 = \bar{k}_2 = 1$ give rise to six distinct f-tilings, whose planar and 3D representations are given in Figures 7–12, respectively.

2. Suppose now that $\alpha > \beta$. As mentioned before, we have $\beta = \delta = \frac{\pi}{2} = a = f$, and consequently $\alpha > \beta = \frac{\pi}{2}$. Analogously to the previous case, the configuration illustrated in Figure 2–A is extended to the one given in Figure 3.

At vertices v_1 and v_2 (in antipodal positions), we must have $\alpha + k\gamma = \pi$, $k \geq 1$. For each $\gamma \in \left(0, \frac{\pi}{2k}\right)$ and $k \geq 1$, the condition $\alpha + k\gamma = \pi$ leads to a class of $\left\lceil \frac{k+1}{2} \right\rceil$ f-tilings, where $\lceil n \rceil$ denotes the smallest integer greater than or equal to n. This class is a subset of $\left\{\mathcal{P}^{\alpha}_{j_{(k_1,k_2)}}\right\}$, with $k_1 \geq 1$ and $k_2 = 1$, and where the roles of α and γ are interchanged. $\square$

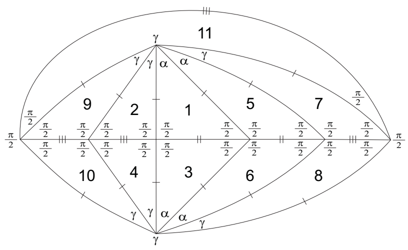

(a) Planar representation of $\mathcal{P}^{\alpha}_{1_{(1,2)}}$

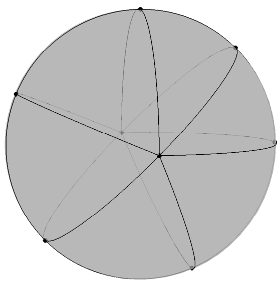

(b) 3D representation of $\mathcal{P}^{\alpha}_{1_{(1,2)}}$

Fig. 5 f-tiling $\mathcal{P}^{\alpha}_{1_{(1,2)}}$, $\alpha \in \left(0, \frac{\pi}{2}\right)$

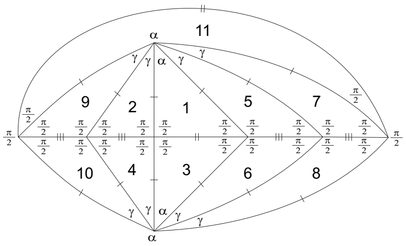

(a) Planar representation of $\mathcal{P}^{\alpha}_{2_{(1,2)}}$

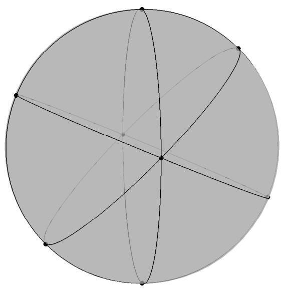

(b) 3D representation of $\mathcal{P}^{\alpha}_{2_{(1,2)}}$

Fig. 6 f-tiling $\mathcal{P}^{\alpha}_{2_{(1,2)}}$, $\alpha \in \left(0, \frac{\pi}{2}\right)$, $\alpha \neq \gamma$

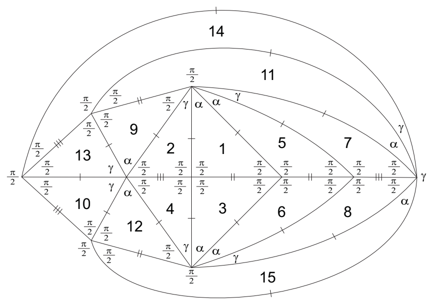

(a) Planar representation of $\bar{\mathcal{P}}^{\alpha}_{1_{(1,1)}}$

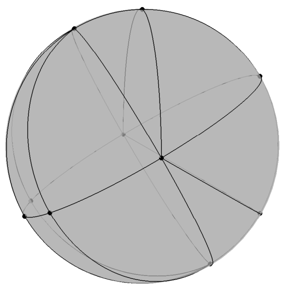

(b) 3D representation of $\bar{\mathcal{P}}^{\alpha}_{1_{(1,1)}}$

Fig. 7 f-tiling $\bar{\mathcal{P}}^{\alpha}_{1_{(1,1)}}$, $\alpha \in \left(0, \frac{\pi}{2}\right)$, $\alpha \neq \gamma$

2.1.2 $b = c$

The condition $b = c$ leads to $\alpha = \frac{\pi}{2} = b = c$ and $\beta = a$. We also have $e \neq a, b, f$ ($e = b$ implies $T_1 \equiv T_2$) and $f \neq a, b$ ($f = a$ implies $\beta = \frac{\pi}{2}$). We will consider separately the subcases $\alpha < \beta$ and $\alpha > \beta$.

Proposition 3. *If there are two cells in adjacent positions as illustrated in Figure 2–A, with $b = c$ and $\alpha < \beta$, then $\Omega(T_1, T_2) = \emptyset$.*

Proof.

Suppose that any element of $\Omega(T_1, T_2)$ has at least two cells congruent, respectively, to T_1 and T_2, such that they are in adjacent positions as illustrated in Figure 2–A, with $\alpha < \beta$. With the labelling used in Figure 13, we have $\theta_1, \theta_2 \in \left\{\beta, \frac{\pi}{2}\right\}$. Nevertheless, as $\beta > \alpha = \frac{\pi}{2}$, we get an impossibility at vertex v. □

Proposition 4. *If there are two cells in adjacent positions as illustrated in Figure 2–A, with $b = c$ and $\alpha > \beta$, then $\Omega(T_1, T_2) \neq \emptyset$ iff*

(i) $\alpha = \frac{\pi}{2}$, $\beta = \frac{\pi}{4} = \gamma$ and $\delta = \frac{\pi}{3}$ or
(ii) $\alpha = \frac{\pi}{2}$, $\beta + \gamma = \frac{\pi}{2}$ and $k\delta = \pi$, with $k \geq 3$.

The first case leads to two different dihedral f-tilings denoted by $\mathcal{S}$ and $\mathcal{T}$, respectively. Planar and 3D representations of $\mathcal{S}$ and $\mathcal{T}$ are given in Figure 17 and Figure 18, respectively.

In the last case, for each $k \geq 3$, we obtain a single tiling, denoted by $\mathcal{R}^k$, with $\beta = \arccos\sqrt{\cos\frac{\pi}{k}}$ and $\gamma = \frac{\pi}{2} - \beta$. A planar representation of $\mathcal{R}^k$ is given in Figure 19(b) and 3D representations, for $k = 3$ and $k = 4$, are given in Figure 20.

Proof.

Suppose that any element of $\Omega(T_1, T_2)$ has at least two cells congruent, respectively, to T_1 and T_2, such that they are in adjacent positions as illustrated in Figure 2–A, with $\alpha > \beta$. With the labelling used in Figure 14(a), we have $\theta_1 = \delta$ or $\theta_1 = \gamma$.

If $\theta_1 = \delta$ (Figure 14(b)), then $\theta_2 = \beta$ or $\theta_2 = \delta$. But in either cases an incompatibility between sides cannot be avoided around vertex v.

Therefore $\theta_1 = \gamma$ (Figure 15(a)). Analyzing the edge lengths, at vertex v we must have

$$\frac{\pi}{2} + k\gamma = \pi \quad \text{or} \quad \frac{\pi}{2} + k_1\gamma + k_2\beta = \pi,$$

with $k \geq 2$ and $k_1, k_2 \geq 1$.

1. Suppose firstly that $\frac{\pi}{2} + k\gamma = \pi$, with $k \geq 2$ (Figure 15(b)). Note that $\theta_2 = \frac{\pi}{2}$ (tiles 7 and 9) as $\theta_2 = \delta$

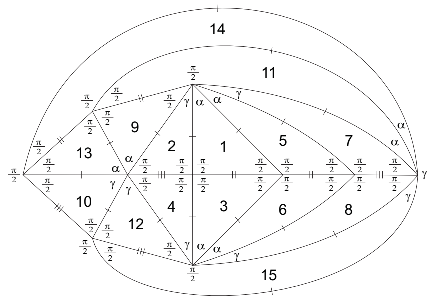

(a) Planar representation of $\bar{\mathcal{P}}^{\alpha}_{2_{(1,1)}}$

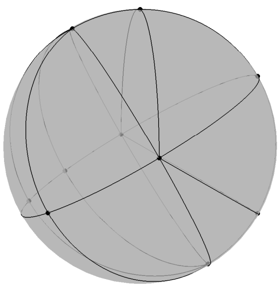

(b) 3D representation of $\bar{\mathcal{P}}^{\alpha}_{2_{(1,1)}}$

Fig. 8 f-tiling $\bar{\mathcal{P}}^{\alpha}_{2_{(1,1)}}$, $\alpha \in \left(0, \frac{\pi}{2}\right)$, $\alpha \neq \gamma$

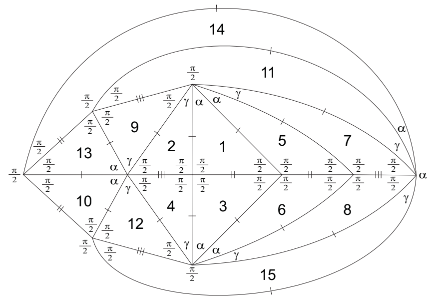

(a) Planar representation of $\bar{\mathcal{P}}^{\alpha}_{3_{(1,1)}}$

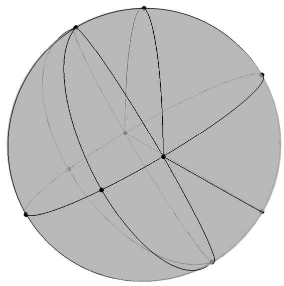

(b) 3D representation of $\bar{\mathcal{P}}^{\alpha}_{3_{(1,1)}}$

Fig. 9 f-tiling $\bar{\mathcal{P}}^{\alpha}_{3_{(1,1)}}$, $\alpha \in \left(0, \frac{\pi}{2}\right)$, $\alpha \neq \gamma$

gives rise to an incompatibility between sides. As $\delta > \frac{\pi}{4}$, at vertex v we have necessarily $2\delta + \gamma = \pi$ or $3\delta = \pi$.

If $2\delta + \gamma = \pi$, we get the local configuration illustrated in Figure 16(a). At vertex v' we must have $\frac{\pi}{2} + \delta + k'\beta = \pi$, for some $k' \geq 1$. Nevertheless, we obtain an impossibility, as an incompatibility between sides cannot be avoided around vertex v'.

If $3\delta = \pi$, i.e., $\delta = \frac{\pi}{3}$, then $\gamma > \frac{\pi}{6}$, and so $\gamma = \frac{\pi}{4}$ ($k = 2$). Moreover, equation (2) implies $\beta = \frac{\pi}{4}$. The last configuration is extended to the one illustrated in Figure 16(b). Now $\theta_3 = \beta$ or $\theta_3 = \frac{\pi}{2}$.

The first case gives rise to a single f-tiling whose planar representation is illustrated in Figure 17(a). We denote such f-tiling by $\mathcal{S}$. The corresponding 3D representation is given in Figure 17(b).

If $\theta_3 = \frac{\pi}{2}$, the last configuration is extended in a unique way to the global planar representation given in Figure 18(a). We denote such f-tiling by $\mathcal{T}$. The corresponding 3D representation is given in Figure 18(b).

2. Suppose now that $\frac{\pi}{2} + k_1\gamma + k_2\beta = \pi$, with $k_1, k_2 \geq 1$.

2.1 We consider firstly the case $k_1 = 1$, i.e., when $\frac{\pi}{2} + \gamma + k_2\beta = \pi$, $k_2 \geq 1$.

2.1.1 If $k_2 = 1$, we obtain the configuration illustrated in Figure 19(a). With the labelling of this figure, we have $\theta_2 = \beta$ or $\theta_2 = \frac{\pi}{2}$.

If $\theta_2 = \beta$, at vertex v_1 we must have $\frac{\pi}{2} + \gamma + \gamma = \pi$, as $\frac{\pi}{2} + \gamma + \beta = \pi$ give rise to an incompatibility between sides. Therefore $\gamma = \beta = \frac{\pi}{4} < \delta$, and consequently at vertex v_2 we get $3\delta = \pi$. The last configuration is then extended in a unique way to a planar representation that corresponds to the previous f-tiling $\mathcal{T}$.

If $\theta_2 = \frac{\pi}{2}$, we get the local configuration illustrated in Figure 19(b). We have $k\delta = \pi$, with $k \geq 3$. Using (2), we obtain $\beta = \arccos\sqrt{\cos\frac{\pi}{k}}$ and $\gamma = \frac{\pi}{2} - \beta$. We denote such family of f-tilings by $\mathcal{R}^k$, $k \geq 3$. The corresponding 3D representations for $k = 3$ and $k = 4$ are given in Figure 20.

2.1.2 If $k_2 \geq 2$ and $\delta \leq \frac{\pi}{4}$, then $\gamma > \frac{\pi}{4}$ and we get the configuration illustrated in Figure 21(a). Note that $\theta_2 = \beta$, as $\theta_2 = \frac{\pi}{2}$ implies $\frac{\pi}{2} + \gamma + k_2\beta = \pi$ and an incompatibility between sides cannot be avoided around vertex v_1. Nevertheless we reach a contradiction at vertex v_2.

On the other hand, if $k_2 \geq 2$ and $\delta > \frac{\pi}{4}$, we have necessarily $3\delta = \pi$ as illustrated in Figure 21(b). If $\theta_2 = \delta$, we reach an incompatibility between sides around vertex v. Now, $\theta_3 = \frac{\pi}{2}$ or $\theta_3 = \beta$. These two distinct cases give rise to the local configurations illustrated in Figure 22(a) and Figure 22(b), respectively. In both cases, at vertex v we must have $\frac{\pi}{2} + k\gamma = \pi$, for some $k \geq 2$. As $\delta = \frac{\pi}{3}$, we have $\gamma > \frac{\pi}{6}$, and so $k = 2$ and $\gamma = \frac{\pi}{4}$. But then,

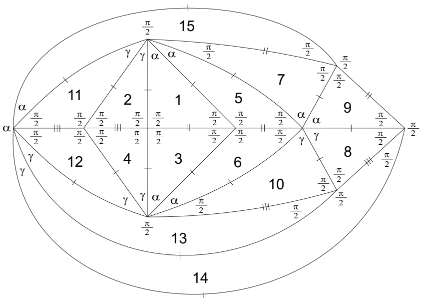

(a) Planar representation of $\bar{\mathcal{P}}^{\alpha}_{4_{(1,1)}}$

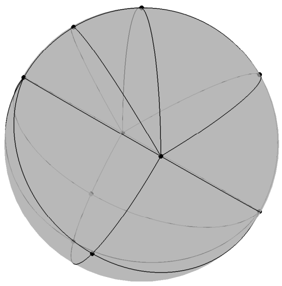

(b) 3D representation of $\bar{\mathcal{P}}^{\alpha}_{4_{(1,1)}}$

Fig. 10 f-tiling $\bar{\mathcal{P}}^{\alpha}_{4_{(1,1)}}$, $\alpha \in \left(0, \frac{\pi}{2}\right)$, $\alpha \neq \gamma$

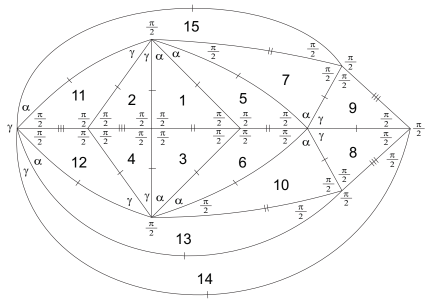

(a) Planar representation of $\bar{\mathcal{P}}^{\alpha}_{5_{(1,1)}}$

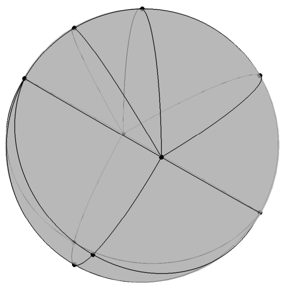

(b) 3D representation of $\bar{\mathcal{P}}^{\alpha}_{5_{(1,1)}}$

Fig. 11 f-tiling $\bar{\mathcal{P}}^{\alpha}_{5_{(1,1)}}$, $\alpha \in \left(0, \frac{\pi}{2}\right)$, $\alpha \neq \gamma$

by equation (2), we conclude that $\beta = \frac{\pi}{4}$, which is not possible since $k_2 \geq 2$.

2.2 If $k_1 \geq 2$, then $\gamma < \frac{\pi}{4} < \delta$ and we get the configuration illustrated in Figure 23(a). Note that $\theta_2 = \gamma$, as $\theta_2 = \delta$ implies $\frac{\pi}{2} + \delta + k\beta = \pi$, for some $k \geq 1$, at vertex v_1, but in this case an incompatibility between sides cannot be avoided around this vertex. Therefore we have $3\delta = \pi$ at vertex v_2, and so $\gamma > \frac{\pi}{6}$. The last configuration is then extended in a unique way to the one given in Figure 23(b). Now, we have $\theta_3 = \beta$ or $\theta_3 = \frac{\pi}{2}$.

In the first case we must have $\frac{\pi}{2} + k\gamma = \pi$, $k \geq 2$, at vertex v_3. As in 2.1.2, we obtain $\beta = \frac{\pi}{4}$, which is not possible.

In the second case we obtain, at vertex v_4, $k\gamma = \pi$, for some $k > 4$. Thus $\gamma = \frac{\pi}{5}$, $\beta = \arccos\sqrt{\frac{2}{5-\sqrt{5}}}$ and $k_1 = 2$. However there is no integer k_2 satisfying $\frac{\pi}{2} + k_1\gamma + k_2\beta = \pi$. $\square$

2.1.3 $b = f$

Proposition 5. *If there are two cells in adjacent positions as illustrated in Figure 2–A and $b = f$, then $\Omega(T_1, T_2) \neq \emptyset$ iff*

(i) $\delta + \alpha + \gamma = \pi$ and $k\beta \geq 3$, $k \geq 3$, or

(ii) $2\alpha + \gamma = \pi$, $\alpha + 3\beta = \pi$ and $\delta = \frac{\pi}{4}$ or

(iii) $\alpha + 2\gamma = \pi$, $\alpha + 2\beta = \pi$ and $\delta = \frac{\pi}{3}$ or

(iv) $\alpha + \gamma + \frac{\pi}{2} = \pi$, $\beta = \frac{\pi}{4}$ and $\delta = \frac{\pi}{3}$ or

(v) $2\alpha + 2\gamma = \pi$, $\alpha + \gamma + 2\beta = \pi$ and $\delta = \frac{\pi}{3}$.

For each $k \geq 3$, the first case leads to a single f-tiling, denoted by $\mathcal{V}^k$. A planar representation is given in Figure 30. 3D representations for $k = 3$ and $k = 4$ are given in Figure 31.
The case (ii) leads to a single f-tiling, denoted by $\mathcal{Z}$. In Figure 38(b) and Figure 39 are given the corresponding planar and 3D representations.
The case (iii) leads to a single f-tiling, denoted by $\mathcal{L}$, whose planar and 3D representations are presented in Figure 42.
The case (iv) leads to a single f-tiling, denoted by $\bar{\mathcal{U}}$, whose planar and 3D representations are presented in Proposition Figure 50(a) and Figure 50(b), respectively.
In the last situation, there is a single f-tiling, denoted by $\mathcal{U}$. In Figure 44 are given the corresponding planar and 3D representations.

Proof.
Suppose that any element of $\Omega\,(T_1, T_2)$ has at least two cells congruent, respectively, to T_1 and T_2, such that they

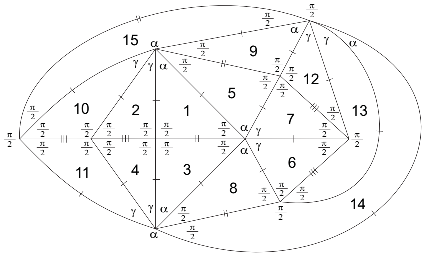

(a) Planar representation of $\bar{\mathcal{P}}^{\alpha}_{6_{(1,1)}}$

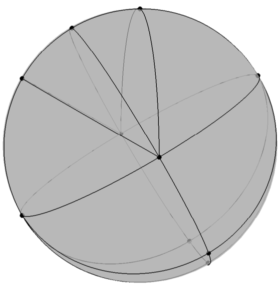

(b) 3D representation of $\bar{\mathcal{P}}^{\alpha}_{6_{(1,1)}}$

Fig. 12 f-tiling $\bar{\mathcal{P}}^{\alpha}_{6_{(1,1)}}$, $\alpha \in \left(0, \frac{\pi}{2}\right)$, $\alpha \neq \gamma$

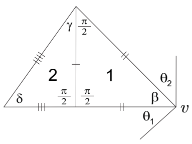

Fig. 13 Local configuration

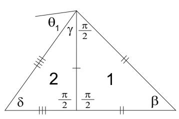

(a)

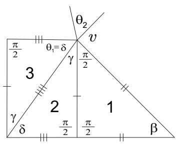

(b)

Fig. 14 Local configurations

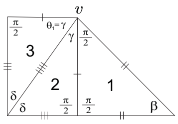

(a)

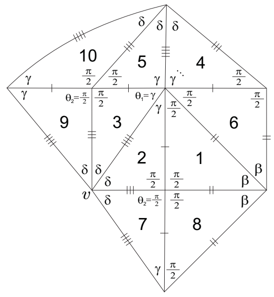

(b)

Fig. 15 Local configurations

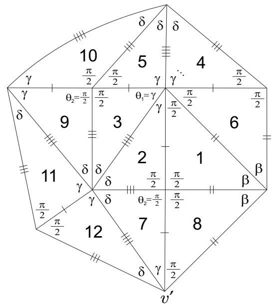

(a)

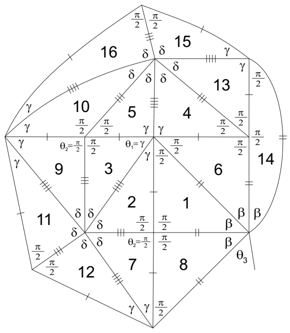

(b)

Fig. 16 Local configurations

are in adjacent positions as illustrated in Figure 2–A. If $b = f$, then

$$\cos\alpha = \cos\beta\cos\gamma \quad \text{and} \quad \sin\beta = \sin\alpha\sin\delta.$$

We also have $e \neq a, b, c$ and $c \neq a, b$.

1. If $\beta > \alpha$, then we must have $\beta > \frac{\pi}{2}$, and consequently $\delta > \frac{\pi}{2}$, otherwise $\sin\alpha < \sin\beta = \sin\alpha\sin\delta$ and $\sin\delta > 1$, which is an incongruence. Therefore we get the configuration illustrated in Figure 24(a). Nevertheless, there is no way to satisfy the angle-folding relation around vertex v.

2. Suppose now that $\beta < \alpha$.

2.1 If $\alpha > \frac{\pi}{2}$, as $\cos\beta\cos\gamma = \cos\alpha < \cos\beta$, we conclude that $\beta < \frac{\pi}{2} < \alpha$, and consequently $\gamma > \frac{\pi}{2} > \delta$. The configuration illustrated in Figure 2–A is then extended in a unique way to the one presented in Figure 24(b). We must have $\alpha + \beta < \pi$ ($\alpha + \beta = \pi$

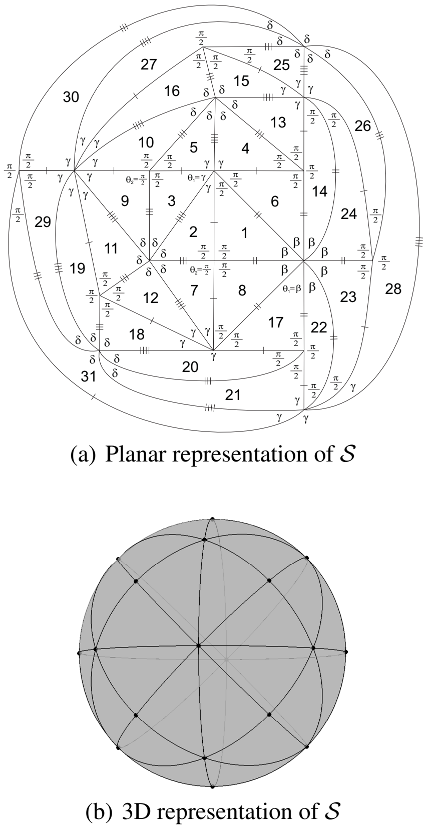

(a) Planar representation of $\mathcal{S}$

(b) 3D representation of $\mathcal{S}$

Fig. 17 f-tiling $\mathcal{S}$

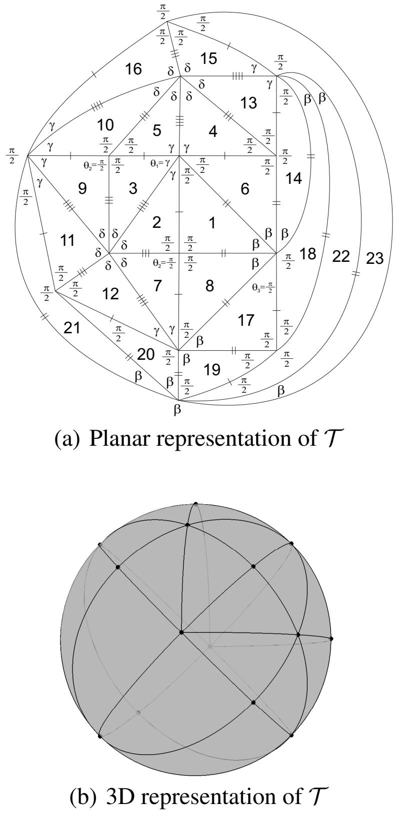

(a) Planar representation of $\mathcal{T}$

(b) 3D representation of $\mathcal{T}$

Fig. 18 f-tiling $\mathcal{T}$

implies $\beta = \frac{\pi}{2}$), but at vertex v there is no way to satisfy the angle-folding relation.

2.2 If $\alpha < \frac{\pi}{2}$, then $\beta < \alpha < \frac{\pi}{2}$ and also $\gamma, \delta < \frac{\pi}{2}$. As $\cos\alpha = \cos\beta\cos\gamma$, we conclude that $\gamma < \alpha$. Moreover, $\sin\beta = \sin\alpha\sin\delta$ implies $\beta < \delta$.

With the labelling of Figure 25(a), we have $\theta_1 = \delta$ or $\theta_1 = \frac{\pi}{2}$.

2.2.1 If $\theta_1 = \delta$ (Figure 25(b)), then at vertex v we must have $\frac{\pi}{2} + k_1\delta + k_2\beta = \pi$, with $k_1 \geq 1$, $k_2 \geq 0$ and $k_1 + k_2 \geq 2$. It is easy to observe that in any choice for k_1 and k_2 an incompatibility between sides cannot be avoided around vertex v.

2.2.2 Suppose now that $\theta_1 = \frac{\pi}{2}$ (Figure 26(a)). Now, we have $\theta_2 = \beta$, $\theta_2 = \delta$ or $\theta_2 = \gamma$.

2.2.2.1 If $\theta_2 = \beta$ (Figure 26(b)), then at vertex v_1 we must have $\alpha + k_1\beta + k_2\gamma = \pi$, with $k_1, k_2 \geq 1$. Note that if at vertex v_1 we have $\alpha+\beta+\alpha = \pi$, $\alpha+k\beta = \pi$ or $\alpha+k_1\beta+k_2\delta = \pi$, $k \geq 2$, $k_1, k_2 \geq 1$, an incompatibility between sides cannot be avoided around this vertex. Moreover, if $\alpha+\beta+\alpha+k\gamma = \pi$, $k \geq 1$, we get $\delta > \alpha > \beta > \gamma$ and consequently a contradiction is achieved at vertex v_2.

Considering the possible angle combinations at vertex v_1, it is easy to observe that the case $k_1 = k_2 = 1$ leads to a contradiction. Therefore $k_1 + k_2 > 2$.

If $\delta > \gamma$, then at vertex v_2 we must have $\frac{\pi}{2} + \delta + k\beta = \pi$, with $k \geq 1$, which implies $\alpha > \delta > \gamma > \beta$. Nevertheless, at vertex v_3 we get $\frac{\pi}{2} + \alpha + \rho > \pi$, $\forall \rho \in \{\frac{\pi}{2}, \alpha, \beta, \gamma, \delta\}$.

Thus, we must have $\alpha > \gamma > \delta > \beta$ and consequently $k_2 = 1$ and $k_1 \geq 2$.

At vertex v_2 (Figure 26(b)) we must have $\frac{\pi}{2} + \bar{k}\delta = \pi$, with $\bar{k} \geq 2$, or $\frac{\pi}{2} + \bar{k}_1\delta + \bar{k}_2\beta = \pi$, with $\bar{k}_1 \geq 2$ and $\bar{k}_2 \geq 1$.

If $\frac{\pi}{2} + \bar{k}\delta = \pi$, $\bar{k} \geq 2$ (Figure 27(a)), then at vertex v_4 we have $\alpha + \alpha + \rho = \pi$, with $\rho \in \{\alpha, \gamma, \delta, \beta\}$. If $\rho = \beta$ (Figure 27(b)), we reach a contradiction at vertex v_5. For the remaining cases, the system (3) is impossible. Note that $\rho = \alpha$ implies $k_1 = \bar{k} = 2$, $\rho = \gamma$ implies $\bar{k} = 2$ and $\rho = \delta$ implies $k_1 = 2$.

$$\begin{cases} \cos\beta\sin\gamma = \cos\delta\sin\alpha \\ \cos\alpha = \cos\beta\cos\gamma \\ \sin\beta = \sin\alpha\sin\delta \end{cases} \quad (3)$$

If $\frac{\pi}{2} + \bar{k}_1\delta + \bar{k}_2\beta = \pi$, with $\bar{k}_1 \geq 2$ and $\bar{k}_2 \geq 1$ (Figure 28(a)), at vertex v_5 we get a contradiction, as for

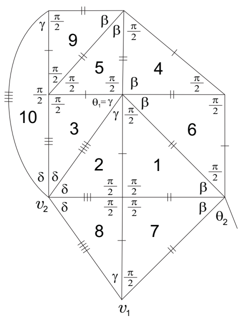

(a)

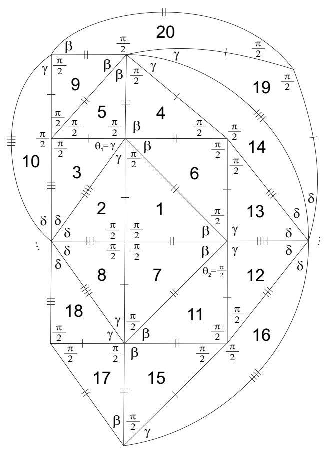

(b) Planar representation of $\mathcal{R}^k$, $k \geq 3$

Fig. 19 Local configurations

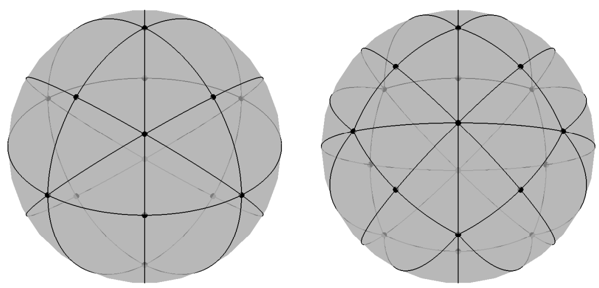

Fig. 20 f-tilings $\mathcal{R}^k$, cases $k = 3$ and $k = 4$

$\rho \in \{\alpha, \gamma\}$, we have $\pi + \pi \geq \left(\frac{\pi}{2} + \delta + \delta + \beta\right) + (\alpha + \alpha + \rho) = \frac{\pi}{2} + (\alpha + \beta) + (\rho + \delta) + (\alpha + \delta) > 2\pi$.

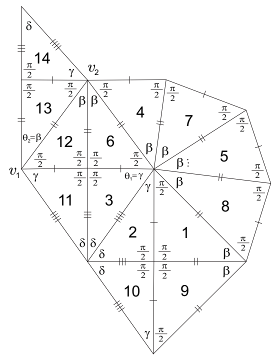

(a)

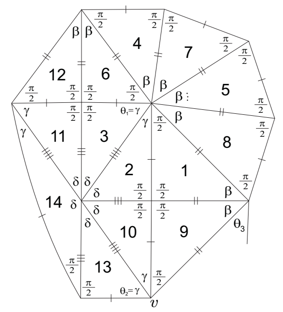

(b)

Fig. 21 Local configurations

2.2.2.2 If $\theta_2 = \delta$ (Figure 28(b)), then at vertex v_1 we must have $\alpha + \delta + k\gamma = \pi$, with $k \geq 1$. Note that if at vertex v_1 we have $\alpha + \delta + \frac{\pi}{2} = \pi$, then $\frac{\pi}{2} + \gamma + \beta = \pi$, which implies that system (3) is impossible. On the other hand, if $\alpha + \delta + \alpha = \pi$ or $\alpha + k_1\delta + k_2\beta = \pi$, $k_1 \geq 1$, $k_2 \geq 0$, $k_1 + k_2 \geq 2$, an incompatibility between sides cannot be avoided around this vertex.

With the labelling of Figure 29(a), we have $(\theta_3, \theta_4) = (\delta, \delta)$, $(\theta_3, \theta_4) = (\delta, \frac{\pi}{2})$, $(\theta_3, \theta_4) = (\frac{\pi}{2}, \delta)$ or $(\theta_3, \theta_4) = (\frac{\pi}{2}, \frac{\pi}{2})$.

(i) If $(\theta_3, \theta_4) = (\delta, \delta)$ (Figure 29(b)), then

- if $\delta > \gamma$, at vertex v_4 we must have $\frac{\pi}{2} + \delta + \bar{k}\beta = \pi$, $\bar{k} \geq 1$. But an incompatibility between sides cannot be avoided around this vertex;
- if $\delta < \gamma$, at vertex v_5 we must have $\frac{\pi}{2} + \gamma + \beta = \pi = \delta + \alpha + \gamma$, which implies that system (3) has no solution.

(ii) If $(\theta_3, \theta_4) = (\delta, \frac{\pi}{2})$ (Figure 29(a)), we consider the subcases $k = 1$ and $k > 1$.

If $k = 1$, we get the local configuration illustrated in Figure 30, where $\bar{k}\beta = \pi$, with $\bar{k} \geq 3$. We denote such family of f-tilings by $\mathcal{V}^k$, $k \geq 3$. The corresponding 3D representations for $k = 3$ and $k = 4$ are given in Figure 31.

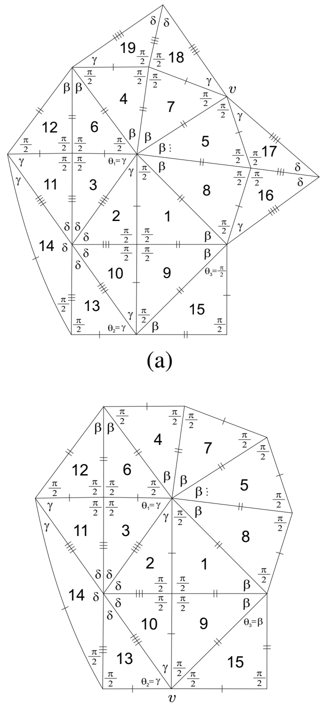

(a) (b)

Fig. 22 Local configurations

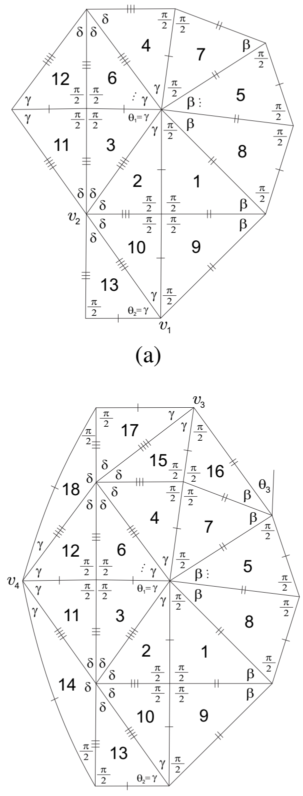

(a) (b)

Fig. 23 Local configurations

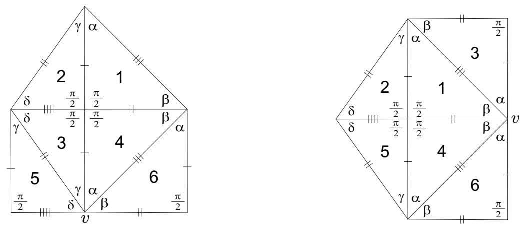

(a) (b)

Fig. 24 Local configurations

If $k > 1$ (Figure 32(a)), then $\delta > \alpha > \beta > \gamma$ and $\delta > \frac{\pi}{4}$. At vertex v_5 we have necessarily $\delta + \delta + \rho = \pi$, with $\rho \in \{\alpha, \beta, \gamma, \delta\}$. In all these cases, and for the possible values of k, we obtain a solution of system (3). Nevertheless, we get a contradiction at vertex v_6, as there is no way to satisfy the angle-folding relation around this vertex.

(iii) Consider now $(\theta_3, \theta_4) = (\frac{\pi}{2}, \delta)$ (Figure 32(b)). If $k = 1$ the system (3) is impossible (at vertex v_1 we have $\delta + \alpha + \gamma = \pi = \frac{\pi}{2} + \gamma + \beta$). The case $k > 1$ leads to a contradiction at vertex v_4, as $\frac{\pi}{2} + \delta + \rho > \pi$, $\forall \rho \in \{\alpha, \beta, \gamma, \delta\}$.

(iv) Observing Figure 33(a) we conclude that in the case $(\theta_3, \theta_4) = (\frac{\pi}{2}, \frac{\pi}{2})$ we get a contradiction at vertex v_4.

2.2.2.3 Finally we analyze the case $\theta_2 = \gamma$ (Figure 33(b)), considering separately the cases $\gamma > \delta$ and $\gamma < \delta$.

2.2.2.3.1 If $\gamma > \delta$ ($\alpha > \gamma > \delta > \beta$), then at vertex v_1 we must have $\alpha + \gamma + \gamma = \pi$, $\alpha + \gamma + \alpha = \pi$, $\alpha + \gamma + \delta = \pi$ or $\alpha + \gamma + k\beta = \pi$, $k \geq 1$.

(i) Suppose firstly that $\alpha + \gamma + \gamma = \pi$, as illustrated in Figure 34(a). At vertex v_2 we have one of the following conditions:

(i1) $\frac{\pi}{2} + \delta + \delta = \pi$;
(i2) $\alpha + \delta + \delta + \beta = \pi$;
(i3) $\gamma + \delta + \delta + \delta = \pi$;
(i4) $\alpha + \delta + \delta + \delta = \pi$;
(i5) $\gamma + \delta + \delta + k\beta = \pi, \ \ k \geq 1$;
(i6) $k_1\delta + k_2\beta = \pi, \ \ k_1 \geq 2, \ \ k_2 \geq 0, \ \ k_1 + k_2 > 3$.

Each one of the conditions (i1)–(i3), jointly with $\alpha + \gamma + \gamma = \pi$, give rise to a solution of the system (3). But with these solutions we obtain a contradiction at vertex v_3, as there is no way to satisfy the angle-folding relation around this vertex.

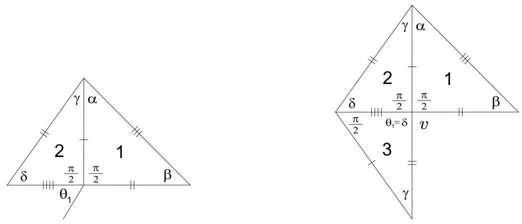

(a) (b)

Fig. 25 Local configurations

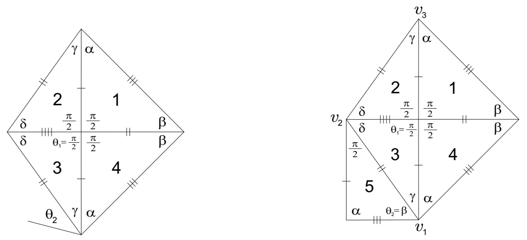

(a) (b)

Fig. 26 Local configurations

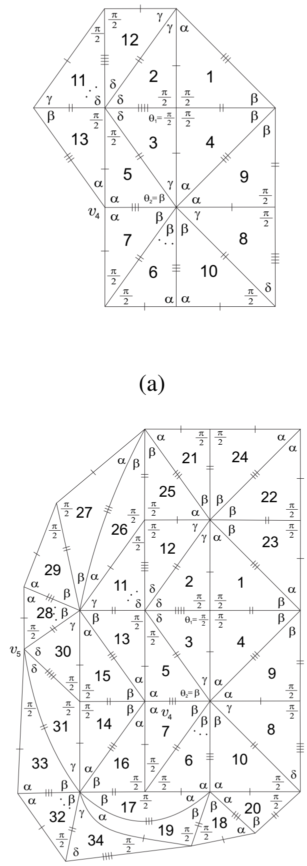

(a)

(b)

Fig. 27 Local configurations

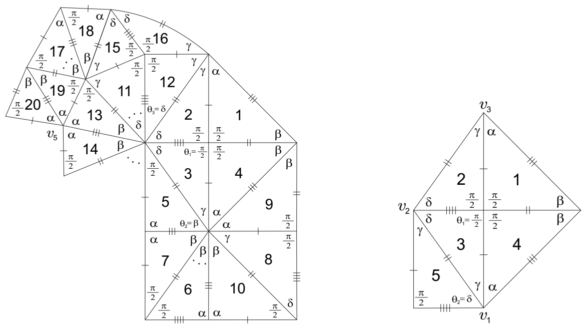

(a) (b)

Fig. 28 Local configurations

The condition (i4) implies that at vertex v_2 we must have $\alpha+\delta+\delta+\delta=\pi=\frac{\pi}{2}+\delta+\delta+\beta$, which leads to an impossible system (3).

If condition (i5) holds then we get the configuration illustrated in Figure 34(b). Note that θ_3 must be γ, otherwise $\theta_4=\frac{\pi}{2}$ and $\frac{\pi}{2}+\alpha+\rho>\pi$, $\forall\rho\in\{\alpha,\beta,\delta,\gamma\}$. At vertex v_4 we have necessarily $\frac{\pi}{2}+\gamma+\bar{k}\beta=\pi$, $\bar{k}\geq 1$, and so the system (3) becomes impossible.

Due to the angles relations and the system (3), if $k_2=0$ in condition (i6), then k_1 must be 5 and we obtain the local configuration illustrated in Figure 35(a). But we get a contradiction at vertex v_3 as there is no way to satisfy the angle-folding relation around this vertex. If $k_2>0$ (Figure 35(b)), then at vertex v_3 we must have $\alpha+\alpha+\rho=\pi$, with $\rho\in\{\beta,\delta\}$. But in either cases an incompatibility between sides cannot be avoided around this vertex.

(ii) If $\alpha+\gamma+\alpha=\pi$ (Figure 36(a)), then at vertex v_2 we have one of the conditions (i1)–(i6) considered in the previous case.

If condition $\frac{\pi}{2}+\delta+\delta=\pi$ (i1) holds, then we obtain one of the configurations illustrated in Figure 36(b) and Figure 37(a). In both cases we get a contradiction at vertex v_3, as an incompatibility between sides cannot be avoided around this vertex (note that, due to the solution of system (3), in the first case at vertex v_3 we must have $\frac{\pi}{2}+\delta+\delta=\pi$ and in the second $\alpha+\beta+\beta+\beta=\pi$).

If $\alpha+\delta+\delta+\beta=\pi$ (Figure 37(b)), then we obtain an impossibility at vertex v_3, since $\frac{\pi}{2}+\alpha+\rho>\pi$, $\forall\rho\in\{\alpha,\beta,\delta,\gamma\}$.

If $\gamma+\delta+\delta+\delta=\pi$, $\alpha+\delta+\delta+\delta=\pi$ or $\gamma+\delta+\delta+\beta=\pi$ (i3)–(i5), then, due to the solution of system (3) for each case, we get a contradiction at vertex v_3 (Figure 36(a)).

If $k_1\delta+k_2\beta=\pi$, $k_1\geq 2$, $k_2\geq 0$, $k_1+k_2>3$ (i6), then, taking into account the vertices v_2–v_4 (Figure 36(a))

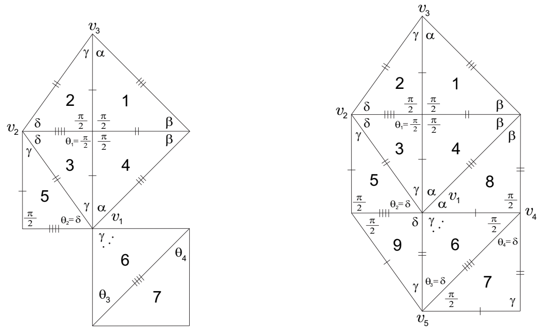

(a) (b)

Fig. 29 Local configurations

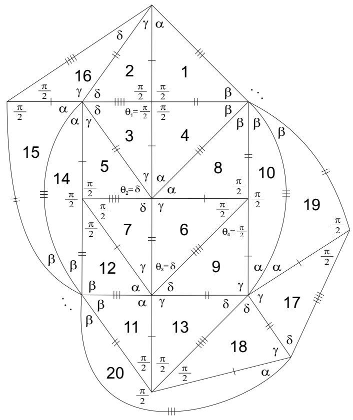

Fig. 30 Planar representation of $\mathcal{V}^k$, $k \geq 3$

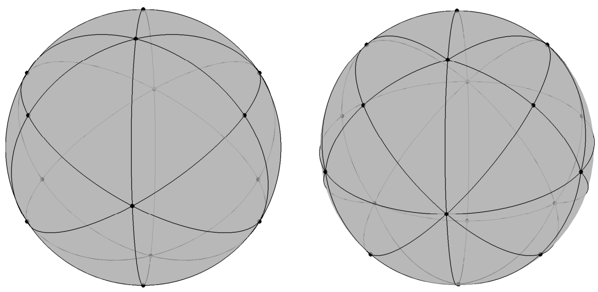

Fig. 31 f-tilings $\mathcal{V}^k$, cases $k = 3$ and $k = 4$

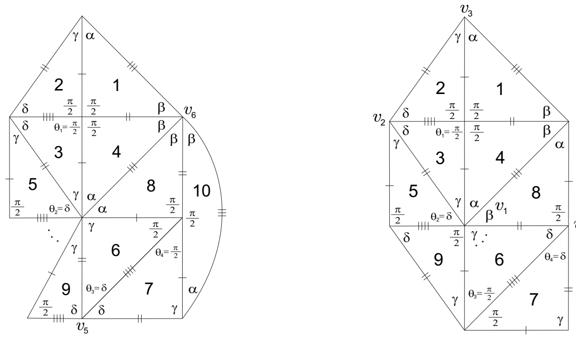

(a) (b)

Fig. 32 Local configurations

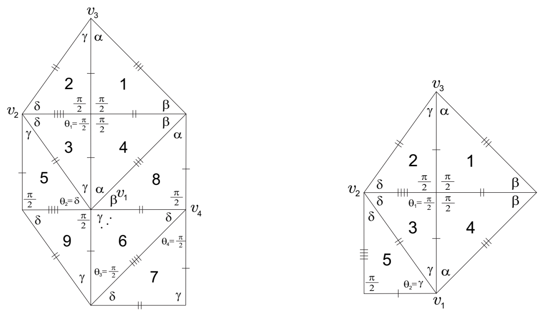

(a) (b)

Fig. 33 Local configurations

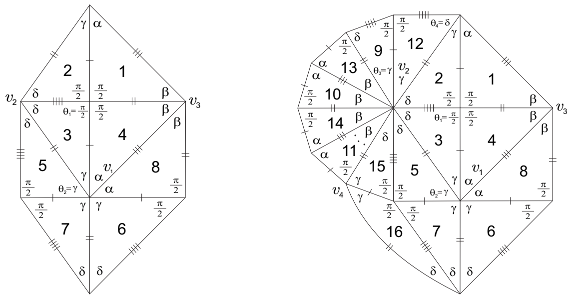

(a) (b)

Fig. 34 Local configurations

and the solutions of system (3), we have ($k_1 = 3$ and $k_2 = 2$) or ($k_1 = 4$ and $k_2 = 0$). The first case leads to a contradiction, as illustrated in Figure 38(a) (at vertex v_4 we have $\frac{\pi}{2} + \alpha + \rho > \pi$, $\forall \rho \in \{\alpha, \beta, \delta, \gamma\}$). The second case give rise to a single f-tiling whose planar representation is illustrated in Figure 38(b). We denote such f-tiling by $\mathcal{Z}$. The corresponding 3D representation is given in Figure 39.

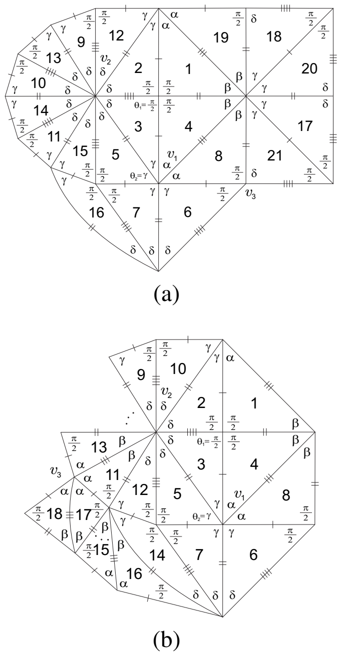

Fig. 35 Local configurations

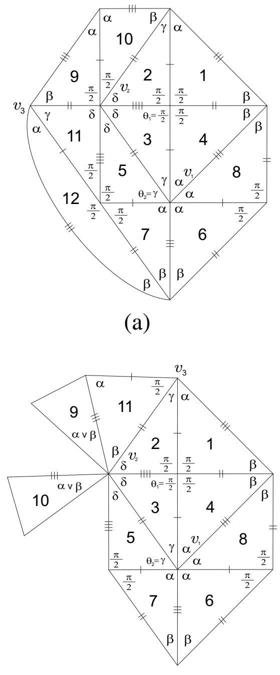

Fig. 37 Local configurations

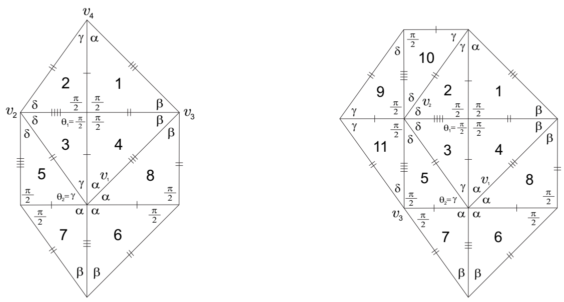

Fig. 36 Local configurations

(iii) If at vertex v_1 (Figure 33(b)) we have $\alpha+\gamma+\delta=\pi$, then we get $\frac{\pi}{2}+\beta+\gamma=\pi$, which implies that system (3) has no solution.

(iv) Finally, if $\alpha+\gamma+k\beta=\pi$, $k\geq 1$ (Figure 40(a)), and considering the possibilities for θ_3, we have $\theta_4=\delta$ or $\theta_4=\frac{\pi}{2}$ (recall that $\frac{\pi}{2}+\alpha+\rho>\pi, \forall\rho\in\{\alpha,\beta,\delta,\gamma\}$).

If $\theta_4=\delta$, then $\theta_3=\delta$ and there is no way to satisfy the angle-folding relation around vertex v_2.

The case $\theta_4=\frac{\pi}{2}$, as illustrated in Figure 40(b), is analogous to the one studied in 2.2.2.2 (ii), where the roles of the angles (α,β) and (γ,δ) are interchanged.

2.2.2.3.2 If $\gamma<\delta$, with the labelling of Figure 33(b), at vertex v_2 we must have one of the following conditions:

(i1) $\delta+\delta+\alpha=\pi$;
(i2) $\delta+\delta+\delta=\pi$;
(i3) $\delta+\delta+\delta+k\beta=\pi,\ \ k\geq 1$;
(i4) $\delta+\delta+\gamma=\pi$;
(i5) $\delta+\delta+\gamma+k\beta=\pi,\ \ k\geq 1$;
(i6) $\delta+\delta+k\beta=\pi,\ \ k\geq 1$.

If condition (i1) holds, then at vertex v_2 (Figure 33(b)) we have $\alpha+\gamma+\delta=\pi=\frac{\pi}{2}+\delta+\beta$, which implies that system (3) has no solution.

In the case (i2) (Figure 41(a)), we have to consider at vertex v_1 the following possibilities:

(j1) $\alpha+\gamma+\frac{\pi}{2}=\pi$;
(j2) $\alpha+\gamma+\alpha=\pi$;
(j3) $\alpha+\gamma+\alpha+\alpha=\pi$;
(j4) $\alpha+\gamma+\delta+\gamma=\pi$;
(j5) $\alpha+\gamma+\alpha+\gamma=\pi$;
(j6) $\alpha+\gamma+\alpha+\beta=\pi$;
(j7) $\alpha+\gamma+k\gamma=\pi,\ \ k\geq 1$;
(j8) $\alpha+\gamma+\gamma+\beta=\pi$;
(j9) $\alpha+\gamma+\delta=\pi$;
(j10) $\alpha+\gamma+k\beta=\pi,\ \ k\geq 1$.

Both conditions (i2)–(j1) and (i2)–(j5) imply $\beta=\frac{\pi}{4}$, $\alpha=\arctan\sqrt{2}$, $\gamma=\frac{\pi}{2}-\alpha$ and $\delta=\frac{\pi}{3}$, and lead to one dihedral f-tiling denoted by $\bar{\mathcal{U}}$, whose planar and 3D representations are presented in Proposition 6 (Figure 50(a) and Figure 50(b), respectively), with the roles of the angles (α,γ) and (β,δ) interchanged.

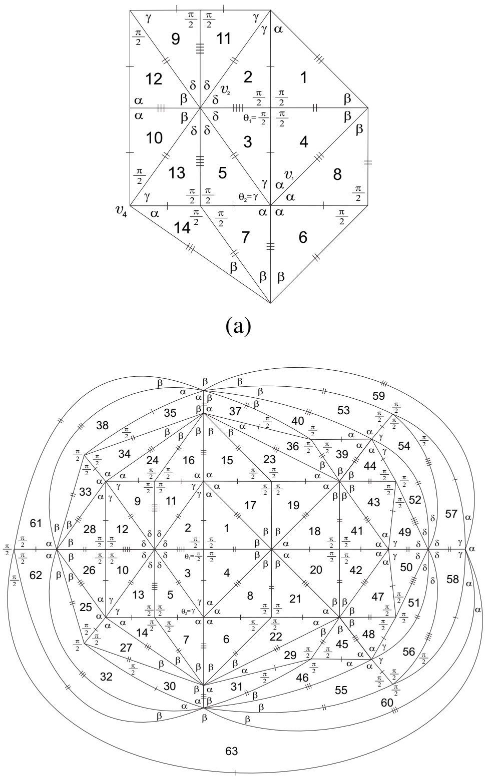

(a)

(b) Planar representation of $\mathcal{Z}$

Fig. 38 Local configurations

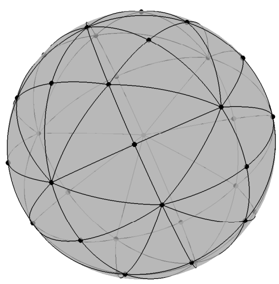

Fig. 39 f-tiling $\mathcal{Z}$

The condition (i2) together with one of the conditions (j2)–(j4) leads to a contradiction at vertex v_4, as we must have a alternating sum containing two angles β and it is not possible due to the respective solutions of system (3).

Also taking into account the solution of system (3) when conditions (i2)–(j6) hold, we obtain a contradiction at vertex v_5 (Figure 41(b)).

If $\alpha+\gamma+k\gamma=\pi$, $k\geq 1$ (j7), then we must have $k=1$ (the other possible values for k lead to a contradiction at vertex v_4, where we have at least two angles β in the

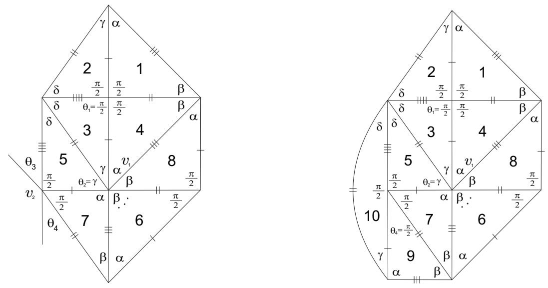

(a) (b)

Fig. 40 Local configurations

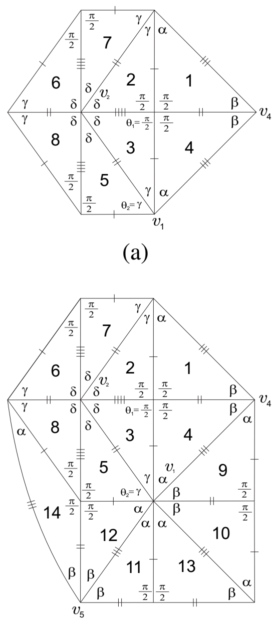

(a)

(b)

Fig. 41 Local configurations

alternated angle sums). In this case we obtain a dihedral f-tiling denoted by $\mathcal{L}$, whose planar and 3D representations are presented in Figure 42.

If condition (j8) holds, then the last configuration extends in a unique way to the one illustrated in Figure 43(a). At vertex v_5 we reach a contradiction since there is no way to satisfy the angle-folding relation.

If condition (j9) holds, then at vertex v_1 (Figure 33(b)) we have $\gamma+\alpha+\delta=\pi=\frac{\pi}{2}+\beta+\gamma$, which implies that system (3) has no solution.

Finally, we consider $\alpha+\gamma+k\beta=\pi$, $k\geq 1$ (j10). If $k=1$, then we obtain the previous f-tiling $\mathcal{L}$. If $k>1$ and $\theta_3=\alpha$ (Figure 43(b)), then $\frac{\pi}{2}+\delta+\bar{k}\beta=\pi$, $\bar{k}\geq 1$, and $\alpha>\delta>\gamma>\beta$. If $\theta_4=\delta$ we obtain a contradiction

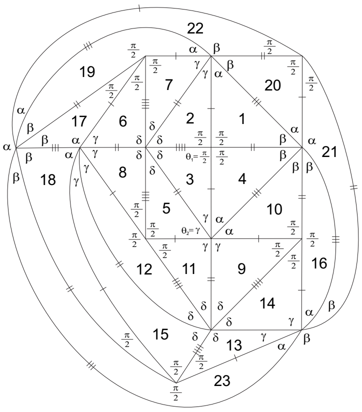

(a) Planar representation of $\mathcal{L}$

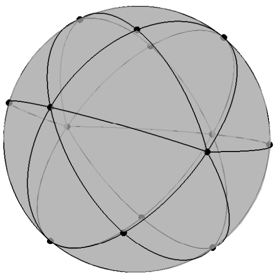

(b) 3D representation of $\mathcal{L}$

Fig. 42 f-tiling $\mathcal{L}$

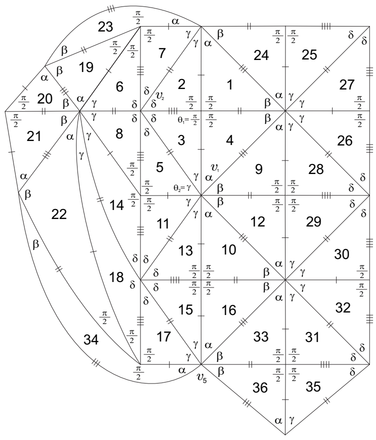

(a)

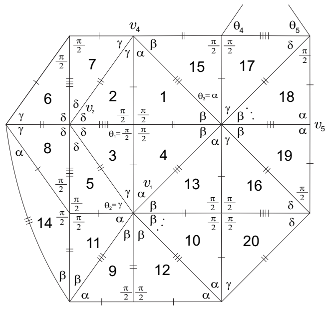

(b)

Fig. 43 Local configurations

at vertex v_4, as $\frac{\pi}{2}+\alpha+\rho>\pi$, $\forall \rho \in \{\frac{\pi}{2},\alpha,\beta,\gamma,\delta\}$. If $\theta_5=\delta$, then at vertex v_5 we have $\alpha+\alpha+\rho=\pi$, with $\rho\in\{\gamma,\beta\}$. But in either cases the system (3) has no solution. The case $\theta_3=\beta$ leads to a dihedral f-tiling denoted by $\mathcal{U}$, whose planar and 3D representations are presented in Figure 44.

In the case (i3) (Figure 45(a)), we have $\alpha>\delta>\gamma>\beta$ and at vertex v_2 we must have $\frac{\pi}{2}+\gamma+\gamma=\pi$, $\frac{\pi}{2}+\gamma+\gamma+\bar{k}\beta=\pi$ or $\frac{\pi}{2}+\gamma+\bar{k}\beta=\pi$, $\bar{k}\geq 1$. In the two first cases, we have $\theta_3=\alpha$ and $\alpha+\alpha+\rho=\pi$, with $\rho\in\{\alpha,\beta,\gamma,\delta\}$. But considering each one of these possibilities for ρ, we conclude that system (3) has no solution. In the last case we obtain $\frac{\pi}{2}+\delta+\bar{\bar{k}}\beta=\pi$, $\bar{\bar{k}}\geq 1$, at vertex v_3 and consequently at vertex v_1 we get $\frac{\pi}{2}+\alpha+\gamma>\pi$.

If $\delta+\delta+\gamma=\pi$ (i4), the last configuration extends to the one illustrated in Figure 45(b). At vertex v_3 we must have $\delta+\alpha+k\beta=\pi$ or $\delta+\alpha+k\gamma=\pi$, $k\geq 1$. For each $k\geq 1$, the condition $\delta+\alpha+k\beta=\pi$ implies that the system (3) is impossible. In the second case, if $k=1$ we obtain the previous f-tiling $\mathcal{L}$; if $k>1$ (Figure 46(a)), as β increases as k increases and $\delta>\alpha>\beta>\frac{\pi}{3}>\gamma$, at vertex v_4 we have necessarily $\beta+\beta+k\gamma$, $k\geq 1$. But an incompatibility between sides cannot be avoided around this vertex.

If condition (i5) holds (Figure 46(b)), then $\alpha>\delta>\gamma>\beta$ and at vertex v_2 we must have $\alpha+\alpha+\rho=\pi$, with $\rho\in\{\alpha,\beta,\gamma,\delta\}$. Any of the choices leads to a system (3) impossible.

Finally, if $\delta+\delta+k\beta=\pi$, $k\geq 1$ (Figure 47), then $\frac{\pi}{2}+\alpha+\gamma=\pi$ and $k=1$. But due to the solution of system (3) a contradiction is achieved at vertex v_3. □

2.2 *Case of Adjacency B*

Suppose that any element of $\Omega(T_1,T_2)$ has at least two cells congruent, respectively, to T_1 and T_2, such that they are in adjacent positions as illustrated in Figure 2–B. As $b=e$, using trigonometric formulas, we obtain

$$\frac{\cos\alpha}{\sin\beta}=\frac{\cos\gamma}{\sin\delta}. \tag{4}$$

In the following subsection we will consider the case $a=f$. The case $c=d$ is analogous interchanging the roles of the angles (α,β) and (γ,δ). The case $a=c$ implies $\sin\beta=1$, and so $\beta=\frac{\pi}{2}=a=c$. It is easy to see that

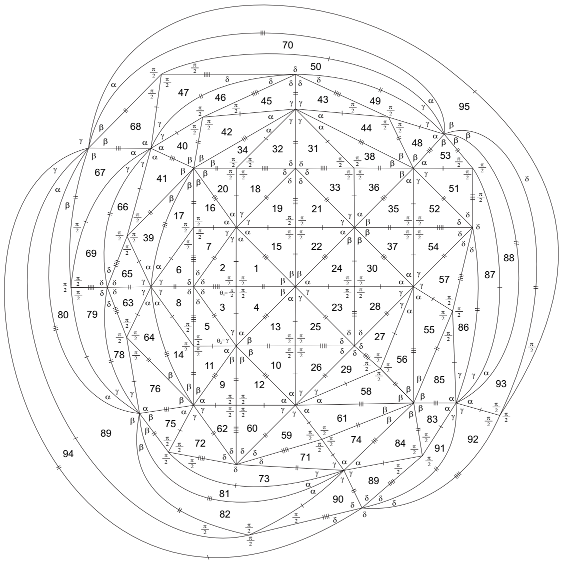

(a) Planar representation of $\mathcal{U}$

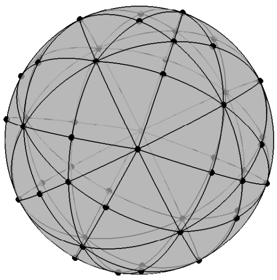

(b) 3D representation of $\mathcal{U}$

Fig. 44 f-tiling $\mathcal{U}$

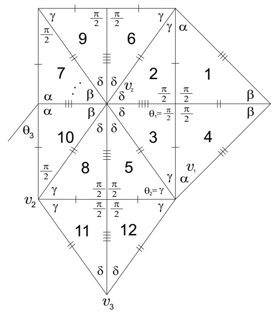

(a)

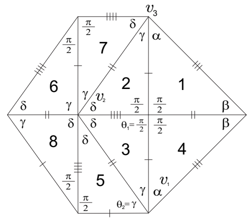

(b)

Fig. 45 Local configurations

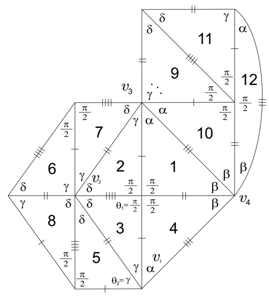

(a)

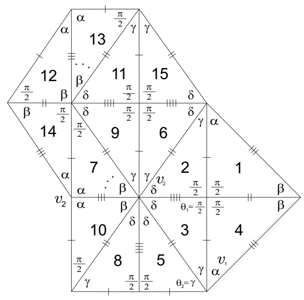

(b)

Fig. 46 Local configurations

the corresponding study is analogous to the one presented in Proposition 3 and Proposition 4 (the same f-tilings are obtained), where the roles of the angles (α, β) and (γ, δ) are interchanged. Both cases $a = d$ and $c = f$ imply $T_1 \equiv T_2$, which is not possible. The cases $b = c$, $c = e$ and $d = f$ are analogous to the case $a = c$. The case $e = f$ implies $b = c$.

2.2.1 $a = f$

If $a = f$, then

$$\cos\beta = \cos\alpha\cos\delta \quad \text{and} \quad \sin\alpha = \sin\beta\sin\gamma.$$

In this case we must have $\alpha < \beta$. In fact, if $\alpha > \beta$ and

(i) $\alpha < \frac{\pi}{2}$, then $\sin\alpha = \sin\beta\sin\gamma > \sin\beta$ and $\sin\gamma > 1$, which is an incongruence.

(ii) $\alpha > \frac{\pi}{2}$, then $\gamma > \frac{\pi}{2}$ (by (4)), and consequently we have $\beta < \frac{\pi}{2} < \delta$ or $\delta < \frac{\pi}{2} < \beta$. In both cases, all the

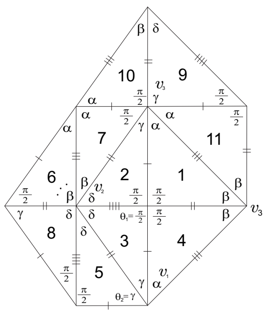

Fig. 47 Local configuration

angles $\alpha, \beta, \gamma, \delta$ are greater than $\frac{\pi}{2}$ except one, which is not possible.

Note that $\alpha \neq \frac{\pi}{2}$, otherwise we get $\alpha = \beta = \frac{\pi}{2}$.

Proposition 6.*If there are two cells in adjacent positions as illustrated in Figure 2–B and $a = f$, then $\Omega(T_1, T_2) \neq \emptyset$ iff $\alpha = \frac{\pi}{4}$, $\beta = \arctan\sqrt{2}$, $\gamma = \frac{\pi}{3}$ and $\delta = \frac{\pi}{2} - \beta$. This conditions lead to one dihedral f-tiling denoted by $\bar{\mathcal{U}}$, whose planar and 3D representations are given in Figure 50(a) and Figure 50(b), respectively.*

Proof.

Suppose that any element of $\Omega\,(T_1, T_2)$ has at least two cells congruent, respectively, to T_1 and T_2, such that they are in adjacent positions as illustrated in Figure 2–B and $a = f$ $(\alpha < \beta)$.

With the labelling used in Figure 48(a), we have $\theta_1 = \frac{\pi}{2}$ or $\theta_1 = \gamma$.

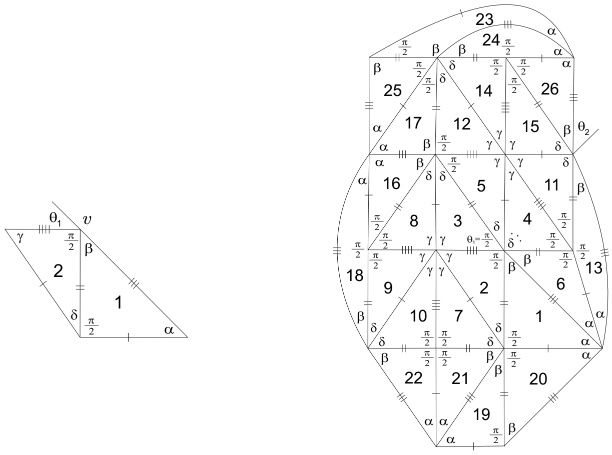

(a) (b)

Fig. 48 Local configurations

1. If $\theta_1 = \frac{\pi}{2}$, then $\frac{\pi}{2} + \beta + k\gamma = \pi$ or $\frac{\pi}{2} + \beta + k\delta = \pi$, for $k \geq 1$. The first case leads to a contradiction at vertex v (there is no way to satisfy the angle-folding relation around this vertex). The condition $\frac{\pi}{2} + \beta + k\delta = \pi$, $k \geq 1$, leads to $\gamma > \beta > \alpha > \delta$ and to the configuration illustrated in Figure 48(b) (note that $\gamma \neq \frac{\pi}{2}$ and $\frac{\pi}{2} + \gamma + \rho > \pi$, $\forall \rho \in \{\frac{\pi}{2}, \alpha, \beta, \gamma, \delta\}$; for instance, tile 7 is a consequence of these conditions). We have necessarily $\gamma = \frac{\pi}{3}$, and so $k = 1$, $\alpha = \frac{\pi}{4}$, $\delta = \operatorname{arccot}\sqrt{2}$ and $\beta = \frac{\pi}{2} - \delta = \arctan\sqrt{2}$.

Now, $\theta_2 = \alpha$ or $\theta_2 = \beta$. In the first case, the last configuration extends in a unique way to the one illustrated in Figure 49. At vertex v we reach a contradiction, as, due

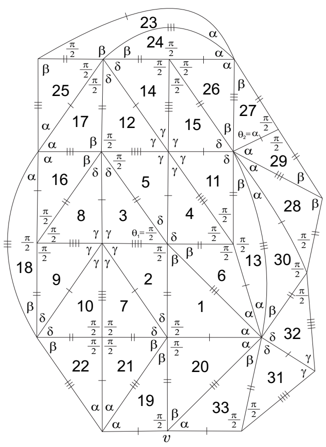

Fig. 49 Local configuration

to the edge lengths, there is no way to satisfy the angle-folding relation around this vertex.

The second case gives rise to a single f-tiling whose planar representation is illustrated in Figure 50(a). We denote such f-tiling by $\bar{\mathcal{U}}$. The corresponding 3D representation is given in Figure 50(b).

2. Suppose now that $\theta_1 = \gamma$ (Figure 51(a)). We have $(\theta_2, \theta_3) = (\gamma, \delta)$ or $(\theta_2, \theta_3) = (\delta, \gamma)$.

2.1 Consider that $(\theta_2, \theta_3) = (\gamma, \delta)$. We separate the subcases $\gamma > \delta$ and $\gamma < \delta$.

2.1.1 If $(\theta_2, \theta_3) = (\gamma, \delta)$ and $\gamma > \delta$, then at vertex v_1 we must have $\frac{\pi}{2} + \gamma + k\alpha = \pi$, $k \geq 1$, and consequently $\beta > \gamma > \delta > \alpha$, $\gamma + \gamma + \beta = \pi$ and $k = 1$ (taking into account the edge lengths and the fact that $\gamma + \gamma + \beta + \rho > \pi$, $\forall \rho \in \{\alpha, \beta, \gamma, \delta, \frac{\pi}{2}\}$). As $\sin\alpha = \sin\beta \sin\gamma$, we obtain $\gamma = \frac{\pi}{2}$, $\gamma = \frac{\pi}{4}$ or $\gamma = \frac{3\pi}{4}$, which is not possible (note that $\gamma = \frac{\pi}{4}$ implies $\beta = \frac{\pi}{2}$).

2.1.2 If $(\theta_2, \theta_3) = (\gamma, \delta)$ and $\gamma < \delta$, then at vertex v_2 we have necessarily $\frac{\pi}{2} + \delta + k\alpha = \pi$, $k \geq 1$, and consequently $\beta > \delta > \gamma > \alpha$. Observing Figure 51(b), we have $\theta_4 =$

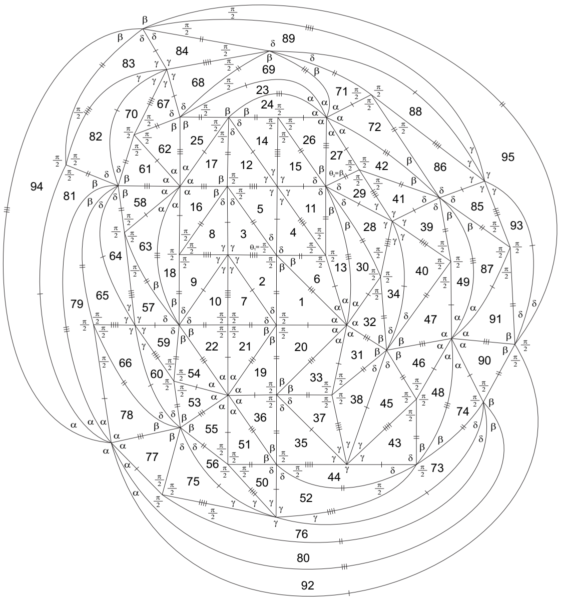

(a) Planar representation of $\bar{\mathcal{U}}$

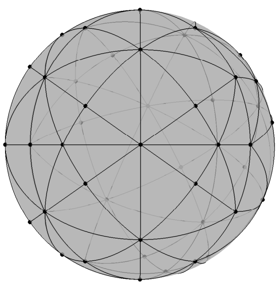

(b) 3D representation of $\bar{\mathcal{U}}$

Fig. 50 f-tiling $\bar{\mathcal{U}}$

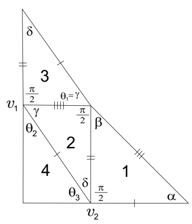

(a)

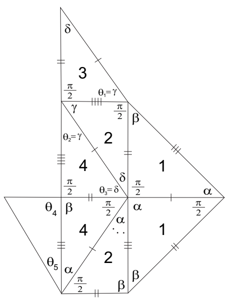

(b)

Fig. 51 Local configurations

β or $\theta_5 = \beta$. In both cases we reach a contradiction, as $\frac{\pi}{2} + \beta + \rho > \pi, \forall \rho \in \{\alpha, \beta, \gamma, \delta, \frac{\pi}{2}\}$.

2.2 Consider now that $(\theta_2, \theta_3) = (\delta, \gamma)$. As in the previous case, we separate the subcases $\gamma > \delta$ and $\gamma < \delta$.

2.2.1 If $(\theta_2, \theta_3) = (\delta, \gamma)$ and $\gamma > \delta$, then at vertex v_2 we must have $\frac{\pi}{2} + \gamma + k\alpha = \pi = \delta + \gamma + k\alpha$, $k \geq 1$, which implies $\delta = \frac{\pi}{2}$, which is not possible.

2.2.2 If $(\theta_2, \theta_3) = (\delta, \gamma)$ and $\gamma < \delta$, then at vertex v_1 we have necessarily $\frac{\pi}{2} + \delta + k\alpha = \pi$, with $k \geq 1$, which implies $\beta > \delta > \gamma > \alpha$. Therefore $k = 1$ and $\frac{\pi}{2} + \delta + \alpha = \pi = \beta + \delta + \gamma$. Solving the system

$$\begin{cases} \cos\beta = \cos\alpha\cos\delta \\ \sin\alpha = \sin\beta\sin\gamma \\ \cos\alpha\sin\delta = \cos\gamma\sin\beta \end{cases},$$

we obtain $\delta = \frac{\pi}{2}$ or $\gamma = \frac{\pi}{2}$, that is not possible. $\square$

3 Summary

In Table 1 is shown a list of the spherical dihedral f-tilings whose prototiles are spherical right triangles (with two pairs of congruent sides in two cases of adjacency), T_1 and T_2, of internal angles $\frac{\pi}{2}$, α, β, and $\frac{\pi}{2}$, γ, δ, respectively. Our notation is as follows:

- $\beta_0^k = \arccos\sqrt{\cos\frac{\pi}{k}}$, $k \geq 3$; $\alpha_1 = \beta_1 = \arctan\sqrt{2}$; α_0^k and δ_0^k are the solutions of system (3), with $k \geq 3$, $\beta = \frac{\pi}{k}$ and $\gamma = \pi - \alpha - \delta$; α_0 is the solution of system (3), with $\beta = \frac{\pi-\alpha}{3}$ and $\gamma = \pi - 2\alpha$.
- $|V|$ is the number of distinct classes of congruent vertices;
- N_1 and N_2 are, respectively, the number of triangles congruent to T_1 and T_2, respectively, used in the dihedral f-tilings.

f-tiling	α	β	γ	δ	$\lvert V\rvert$	N_1	N_2
$\mathcal{P}^{\alpha}_{j(k_1,k_2)}$ $k_1, k_2 \geq 1$	$\left(0, \frac{\pi}{2}\right)$ $\alpha \neq \gamma$	$\frac{\pi}{2}$	$\frac{\pi - k_1\alpha}{k_2}$	$\frac{\pi}{2}$	-	$4k_1$	$4k_2$
$\bar{\mathcal{P}}^{\alpha}_{\bar{j}(\bar{k}_1,\bar{k}_2)}$ $\bar{k}_1, \bar{k}_2 \geq 1$	$\left(0, \frac{\pi}{2}\right)$ $\alpha \neq \gamma$	$\frac{\pi}{2}$	$\frac{\pi - 2\bar{k}_1\alpha}{2\bar{k}_2}$	$\frac{\pi}{2}$	-	$8\bar{k}_1$	$8\bar{k}_2$
$\mathcal{S}$	$\frac{\pi}{2}$	$\frac{\pi}{4}$	$\frac{\pi}{4}$	$\frac{\pi}{3}$	5	8	24
$\mathcal{T}$	$\frac{\pi}{2}$	$\frac{\pi}{4}$	$\frac{\pi}{4}$	$\frac{\pi}{3}$	5	12	12
$\mathcal{R}^k, k \geq 3$	$\frac{\pi}{2}$	β_0^k	$\frac{\pi}{2} - \beta$	$\frac{\pi}{k}$	3	$4k$	$4k$
$\mathcal{V}^k, k \geq 3$	α_0^k	$\frac{\pi}{k}$	$\pi - \delta - \alpha$	δ_0^k	3	$4k$	$4k$
$\mathcal{Z}$	α_0	$\frac{\pi-\alpha}{3}$	$\pi - 2\alpha$	$\frac{\pi}{4}$	4	48	16
$\mathcal{L}$	$\pi - 2\beta$	β_1	β	$\frac{\pi}{3}$	5	12	12
$\mathcal{U}$	α_1	$\frac{\pi}{4}$	$\frac{\pi}{2} - \alpha$	$\frac{\pi}{3}$	5	48	48
$\bar{\mathcal{U}}$	$\frac{\pi}{4}$	β_1	$\frac{\pi}{3}$	$\frac{\pi}{2} - \beta$	5	48	48

Table 1 Combinatorial structure of dihedral f–tilings of S^2 by right triangles

Acknowledgement

The authors acknowledge the financial support from the Portuguese Government through the FCT – Fundação para a Ciência e a Tecnologia, project PEst-OE/MAT/UI4080/2011. The authors are grateful to the anonymous referee for a careful checking of the details and for helpful comments that improved this paper.

References

[1] A. M. Breda, A Class of Tilings of S^2, Geometriae Dedicata, **44**, 241−253 (1992).

[2] A. M. Breda and A. F. Santos, Symmetry Groups of a Class of Spherical Folding Tilings, Applied Mathematics and Information Sciences, **3**, 123−134 (2009).

[3] A. M. Breda, P. S. Ribeiro and A. F. Santos, A class of spherical dihedral f-tilings, *European Journal of Combinatorics*, **30**, 119−132 (2009).

[4] C. P. Avelino and A. F. Santos, Right triangular dihedral f–tilings of the sphere: $\left(\alpha, \beta, \frac{\pi}{2}\right)$ and $\left(\gamma, \gamma, \frac{\pi}{2}\right)$, *Ars Combinatoria*, in press.

[5] C. P. Avelino and A. F. Santos, Right triangular dihedral f–tilings of the sphere: the $\left(\frac{\pi}{2}, \frac{\pi}{4}, \frac{\pi}{3}\right)$, $\left(\frac{\pi}{2}, \frac{\pi}{3}, \frac{\pi}{3}\right)$ family, *Advances and Applications in Discrete Mathematics*, **6**, 139−152 (2010).

[6] S. Robertson, Isometric folding of Riemannian manifolds, *Proceedings of the Royal Society of Edinburgh*, **79**, 275−284 (1977).

[7] R. J. Dawson, Tilings of the sphere with isosceles triangles, *Discrete & Computational Geometry*, **30**, 467−487 (2003).

[8] R. J. Dawson and B. Doyle, Tilings of the sphere with right triangles I: the asymptotically right families, *Electronic Journal of Combinatorics*, **13**, #R48 (2006).

[9] R. J. Dawson and B. Doyle, Tilings of the sphere with right triangles II: the $(1, 3, 2)$, $(0, 2, n)$ family, *Electronic Journal of Combinatorics*, **13**, #R49 (2006).

[10] Y. Ueno and Y. Agaoka, Classification of tilings of the 2-dimensional sphere by congruent triangles, *Hiroshima Mathematical Journal*, **32**, 463−540 (2002).

Catarina P. Avelino is an assistant professor at the Dept. of Mathematics of the University of Trás-os-Montes e Alto Douro, Portugal. She received her Ph.D. degree in mathematics from the University of Coimbra in 2004. She is also a member of the Mathematics Research Unit CM-UTAD and the developed research has been supported by the Portuguese Foundation for Science and Technology. Her current research interests include Geometry (differential and combinatorial) and Topology (isometric foldings on Riemannian manifolds).

Altino F. Santos obtained his Ph.D. in Mathematics (geometry and topology) in 2006, from the University of Trás-os-Montes e Alto Douro, Portugal. He currently works as an assistant professor at the Mathematics Department of University of Trás-os-Montes e Alto Douro. He is also a member of the Mathematics Research Unit CM-UTAD and his current research interests are Geometry (differential and combinatorial) and Topology (isometric foldings on Riemannian manifolds). His research has been supported by the Portuguese Foundation for Science and Technology.